Translation of article 10.22146/jnteti.v13i2.9430

Effects of Codebook Design Weighting on Sparse Code Multiple Access System Performance

Shilvy Fatma Fitria Rachmawati[1], Linda Meylani[1], Vinsensius Sigit Widhi Prabowo[1]

[1] Telecommunication Engineering Study Program, School of Electrical Engineering, Telkom University, Bandung, Jawa Barat 40287, Indonesia

[Submitted: August 31, 2023, Revised: October 17, 2023, Accepted: 18 March 2024]
Corresponding Author: Shilvy Fatma Fitria Rachmawati (email: shilvyfatmafitriar@student.telkomuniversity.ac.id)

ABSTRACT — Sparse code multiple access (SCMA) can support the system when overloading on the receiving side, thereby improving the system's spectral efficiency by designing symbol mapping appropriately. The performance of SCMA is assessed through the utilization of a sparse codebook, wherein bits are directly mapped to multidimensional codewords influenced by both the energy diversity and the minimum Euclidean distance of the multidimensional constellation (M_C). The codebook design simulation was conducted using both Latin and non-Latin generators with phases of 60° and 45°, incorporating weighting values of $w_1 = 0.6$; $w_2 = 0.3$; $w_3 = 0.1$. The simulation also included line constellation with additive white Gaussian noise (AWGN) channel, Rayleigh fading, and Rician channel. This study presented the optimal results across three channels: Latin 60° with BER 10^{-3} in the AWGN channel, non-Latin 60° with BER 10^{-3} in the Rayleigh fading, and non-Latin 45° with BER 10^{-3} in the Rician channel. Then, the results on the codebook design weighting were as follows: Latin 60° with BER 10^{-1} in the AWGN channel, non-Latin 45° with BER 10^{-1} in the Rayleigh fading, and Latin 45° with BER 10^{-3} in the Rician channel. The simulation results state the effect of weighting on each channel. It was found that Latin generators could improve BER performance by suppressing overlap at constellation points and eliminating errors occurred in SCMA codebooks. However, this improvement was observed only in AWGN channels and not for non-Latin generators.

KEYWORDS — Sparse Code Multiple Access, Codebook Design Weighting, Phase Rotation, Base Constellation, BER.

I. INTRODUCTION

The fifth generation (5G) wireless communication is expected to support different user cases, providing strong connectivity, low power consumption, high reliability, and minimal latency [1]. International Data Corporation (IDC) estimates smart devices will increase to 41.6 billion by 2024 [2].

Plural access is a technique used to manage simultaneous access from multiple users to wireless communication resources. The orthogonal multiple access (OMA) scheme eliminates multiuser interference and is compatible with simple transceivers [3]. Examples of OMA schemes include time division multiple access (TDMA), frequency division multiple access (FDMA), and code division multiple access (CDMA) [4]. However, this technique is unable to support 5G systems, which require a vast number of users and devices [5].

The formation of nonorthogonal multiple access (NOMA) [6] has been shown to increase the capacity of wireless communication systems, rendering it a promising technique for 5G wireless communication. Reference [7] asserts that NOMA demonstrates significant multi-user capacity in the additive white Gaussian noise (AWGN) downlink channel. One notable NOMA technique, known as sparse code multiple access (SCMA) [8], was successfully developed in 2013. This technique proves effective in supporting systems during overloading conditions, thereby enhancing spectrum efficiency [9].

SCMA is a nonorthogonal multiple access technique based on the use of codebooks. SCMA performance is influenced by codebook design and the decoding process using a message-passing algorithm (MPA) [10]. The large number of layers on SCMA allows for great connectivity [11], making it suitable for meeting the connectivity requirements of 5G wireless networks.

The design of the codebook influences the bit error rate (BER) value, a process achieved through two steps, firstly, designing a multidimensional constellation (M_C), and secondly, performing specific operations on M_C to generate codebooks [12].

Reference [13] served as the primary source in this study. The study examined SCMA codebooks utilizing constellation rotation and employing both Latin and non-Latin generator matrices. The resulting output was the performance of BER with quadrature modulation phase-shift keying (QPSK) and binary phase-shift keying (BPSK) with phase values set to $\frac{\pi}{3}, \frac{\pi}{4}, \frac{\pi}{5}$, and $\frac{\pi}{6}$ on the AWGN channel.

This study achieved a bit error rate (BER) comparable to that reported in [13] by modifying the line constellation and incorporating weight into the codebook design with phase values of $\frac{\pi}{4}$ and $\frac{\pi}{3}$, and conducting tests on AWGN channels, Rayleigh fading channels, and Rician channels.

This study aimed to design a codebook for the SCMA system and analyze its impact on the measured system performance, specifically the BER. The objectives of this study include determining the effect of the codebook design, evaluating the impact of codebook design weighting, assessing the influence of codebook design weighting on ϕ_0, and examining the effect of phase shifts on the constellation diagram. Additionally, the primary goal is to investigate the effect of weighting on the SCMA codebook design, an aspect that has not been addressed in the main reference.

II. METHODOLOGY

A. SYSTEM MODEL

In an uplink SCMA system, user J is divided into orthogonal resource elements $(RE)_s$-K through the base station (BS). The SCMA encoder functions as a mapping from $\log_2 M$ bits to a K-dimensional complex codebook that is of size M. Each user occupies N orthogonal time-frequency resources, J

is $\binom{K}{N}$, and overloading factor $\lambda = J/K > 1$. Codebooks are sparse and MPA possesses an iterative nature, serving to detect low-complexity multiusers who exploit repeated message exchanges between resource nodes and layer nodes. If the $J = 6$ user shares to $K = 4$ orthogonal RE, the constellation point utilized in the codebook is $M = 4$, with an overloading factor of $\lambda = 150\%$. $F_{4\times6}$ denotes the relationship between the resource and the user. Through the factor graph description, by inserting the K-N row zero elements into the I_N unit matrix and the obtained sparse matrix, V has the same zero-zero row as $F_{4\times6}$.

B. SIMULATION SCHEME

The simulation scheme can be implemented after designing a system that meets the criteria. Figure 1 describes the processes structured in system design to facilitate research.

C. SCMA BASIC CONCEPT

In CDMA systems, as the number of users increases, the resulting detection complexity can increase exponentially on the receiving side. However, studies have shown that this complexity can be effectively reduced when the system is overloaded, meaning when the number of users exceeds available resources. The complexity that arises poses challenges in maintaining system stability on the receiving end, particularly when the factors contributing to overloading are more pronounced.

Building upon the chip sequence design in CDMA, known as sparse spreading, a low-density signature (LDS) was created, originally proposed by Reza Hoshyar [14]. This advancement led to the evolution of CDMA to LDS-CDMA, capable of functioning even under system overload conditions by spreading modulated symbols across nonzero elements of the spreading code [15]. It is achieved due to its extended signature length and multiple nonzero elements, which effectively reduce the complexity of MPA.

To meet the requirements of the 5G system, SCMA was developed as an upgrade to the LDS-CDMA system [16]. In an LDS system**,** bits are directly mapped to the quadrature amplitude modulation (QAM) symbols, repeated, and transmitted through subcarriers based on the specified signature. In contrast, in SCMA bits are directly mapped to multidimensional complex codewords from predetermined codebooks. SCMA does not repeat QAM symbols but instead provides shaping gain through a multidimensional constellation design [17]. One similarity between these two systems is the small number of dimensions required to transmit data, resulting in a very small number of codewords in SCMA.

SCMA is a nonorthogonal plural access technique based on the use of codebooks formed from M_C and shaping gain. SCMA can mitigate interference between users [11] due to the sparse properties of the codebook, which includes a “zero” element in the codeword directly receiving data input. The significant number of layers in SCMA enables extensive connectivity, thereby meeting the connectivity requirements of 5G wireless networks. SCMA serves as a viable solution in scenarios characterized by an increase in users under overloaded conditions.

Codebooks are sparse and can produce optimal BER performance based on symbol mapping results. SCMA performance is influenced by energy diversity and the Euclidean minimum distance from M_C. MPA serves as a user detection algorithm on the receiving side. The SCMA system

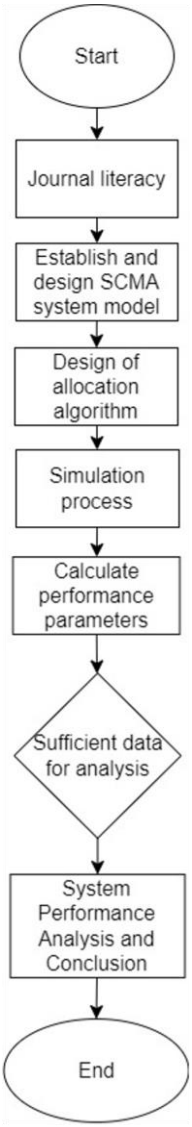

Figure 1. Simulation scheme.

processes begin with bits of information and culminate in the formation of codewords in the system.

The criteria in the SCMA concept are as follows [9].

1. Binary data is encoded into multidimensional codewords from a set of codebooks.
2. A single codebook may be intended for either one user or one layer.
3. Codewords on the formed codebooks are sparse, enabling multi-user detection on MPA to identify multiplexed codewords with adequate complexity.
4. The number of multiplexed layers exceeds the dispersion factor.

The structure of the SCMA codebook is described by the factor graph matrix [8], as expressed by (1).

$$F = (f1, f2, \ldots, fJ) \quad (1)$$

where f_1, f_2, ..., f_J represent the specific user and can be represented in (2) [8].

$$f_j = \text{diag}\,(V_j v_j^T) \quad (2)$$

where V_j is a sparse binary mapping matrix that derives codebooks from multidimensional constellations for each user and v_j^T is a *transpose* matrix from V_j.

The number of users (J) and resource element (K) are connected if and only if $(F)_{KJ} = 1$. The formation of a factor graph matrix for six users in four resource elements, namely $J = 6$, $K = 4$, $N = 2$, and overloading factor (λ) = 0.1. The number of users is determined using (3) [9].

$$J = \binom{K}{N} \quad (3)$$

where N is a nonzero element. The users served in each resource are defined by (4) [9].

$$d_{fJ} = d_f = \binom{K-1}{1} = K - 1. \quad (4)$$

By summing K–N rows of zero elements on an N-size identity matrix, a mapping matrix can be formed.

D. SCMA SYSTEM SCENARIO

The research began with the initiation of system parameters, namely $K = 4$, $N = 2$, $J = 6$, $M = 4$, 4×4 codebook, and the signal frame. Subsequently, data input in the form of bits was generated to iterate signal-to-noise ratio (SNR). These data bits were then mapped to a codeword of 4×4, codebook dimensions, and the constellation was rotated according to the phase. Each user then formulated six mapping matrices, then formed a factor graph matrix that later then be converted into symbolic forms and inputted into the SCMA encoder system, channel propagation, and SCMA decoder. The symbol was then reverted to its initial forms, i.e., bits, and the BER value on the SCMA system was calculated.

E. MULTIDIMENSIONAL CONSTELLATION (M_C)

The design and operation of user-specific M_C served to generate codebooks. M_C was designed and optimized to achieve the maximum value of shaping gain and the value of the farthest normalized Euclidean minimum distance. The minimum Euclidean distance was obtained using (5) [18].

$$dmin = min\{|xi - xi,|, i \neq i'\} \quad (5)$$

where xi is the superposition of codeword elements on resource k that produces M^{df} from $1 \leq i \leq M^{df}$ constellation point where m_{df} values 1, 2, …, df using (6) [19].

$$x_i = x_{m1}^{(K)} + x_{m2}^{(K)} + \cdots + x_{mdf}^{(K)}. \quad (6)$$

The codebook at SCMA was optimized to facilitate the distinction between stacked layers on the resource element, thereby simplifying the decoding process.

Designing a constellation is challenging due to the potential overlap of resource elements across multiple layers. The optimal minimum Euclidean distance from the multidimensional constellation results in good system performance, particularly when the number of layers is minimal and without collisions between layers [20]. As the number of layers increases, so does the likelihood of collisions between them. Consequently, rotation is needed within the constellation to manage dimensional dependencies and power variations while preserving Euclidean distance.

F. FORMATION OF CODEBOOK SCMA

The codebook was constructed by modifying the mapping matrix using a factor graph and selecting parameters for permutation vector and phase rotation operators, influenced by multidimensional constellations, and shaping gain [21]. Each layer of the codebook may be generated to determine the value of the multidimensional constellation and the exact value of the operator. The operator can adjust the average power level in the constellation dimensions, it facilitates the detection of MPA and the separation of interfering symbols. Operators were categorized into three types: complex conjugate operators, phase operators, and permutation vectors.

Codebook optimization was conducted to ensure that each layer within the resource element did not overlap with one another, allowing for clear distinction and facilitating the decoding process. The design of the codebook design had to be carried out by considering the spacing of the points in the constellation and the average energy of the symbols. The average energy of the points in the constellation is represented by (7) [9].

$$E_s = \frac{1}{M^{df}} \sum_{i=1}^{M^{df}} ||x_i||^2. \quad (7)$$

The formation of the codebook commenced by multiplying the values of the mapping matrix, the permutation vector parameters, and the phase rotation operators adjusted to their respective constellation conditions. Subsequently, a permutation operation was conducted on multidimensional constellations to generate the structure of the codebook. This process was computable using (8) [21].

$$x_j = V_j(\Delta_j)\, M\_C \quad (8)$$

where V_j is the mapping matrix; Δ_j may consist of three types, namely phase operators, permutation vectors, and complex conjugates; and M_C is the designed basic constellation form.

Codebook plays a crucial role in replacing modulation and signature schemes in LDS by possessing sparse properties, enabling optimal BER performance through appropriately designed symbol mapping. Factors such as Euclidean minimum distances, the number of collisions at constellation points, and *dmin* pairs also influence the performance of codebook dependent BER systems. Various codebooks utilize the same resource block as sparse "zero" elements in codeword by reducing interference between users.

G. SIMULATION PARAMETERS

Table I shows the parameters that have been set for use in the simulation implementation. Following the main reference [14], this study used the same user, resource element, nonzero element, constellation point, phase rotation, and generation matrix. Modification was carried out using the basic constellation, a range of SNR values, varying lengths of bit data, the addition of weighting values that sum up to 1, and accounting for channel variations. These modifications were implemented to highlight more significant differences.

The Latin generating matrix serves to optimize the codebook structure. For comparison, a non-Latin generator was developed specifically for the SCMA system (4, 6).

Channels serve to design wireless communications and analyze the performance of a system. The AWGN channel, Rayleigh fading, and Rician channel are used to analyze the performance of BER, thus enhancing the accuracy of the system simulation process. AWGN, a natural noise present in communication channels, is utilized to analyze the basic performance of the system against the parameters to be measured. This noise exists on the receiving side and exhibits additive, white, and Gaussian properties. Rayleigh fading in wireless communications illustrates the time variation that alters the natural statistics on the receiver side. It explains the fluctuations of Rayleigh signals in the distribution function of normalized receiving power. On the receiving side, the Rician channel typically features a dominant signal due to line of sight (LOS). The Rician channel in the communication system

TABLE I
SIMULATION PARAMETERS

Parameter	Symbol	Quantity/Type
User (Layer)	*J*	6
Resource element	*K*	4
Non-zero element	*N*	2
Constellation point	*M*	4
Basic constellation	M_C	Line
Phase rotation	Δ	$\frac{\pi}{4}$ and $\frac{\pi}{3}$
Weighting value	*w*	w_1 = 0.6; w_2 = 0.3; and w_3 = 0.1
Generator matrix	-	Latin and non-Latin
Signal-to-noise ratio	SNR	0 – 20 dB
Data length	-	10^7 bit
Channel	-	AWGN, Rayleigh, and Rician

exhibits variance in signal strength, resulting from responses such as reflection, shadowing, and scattering from different environments.

H. METHODOLOGY

The SCMA system model in this study simulated the design of two types of codebook designs, namely codebook design of phase and codebook design of weighting with weight values of w_1 = 0.6; w_2 = 0.3; and w_3 = 0.1, using phase rotation of $\frac{\pi}{4}$ and $\frac{\pi}{3}$, using Latin and non-Latin generators [22], line constellation with AWGN channels, Rayleigh fading, and Rician channels. The measured system performance was BER.

The design of the constellation with constellation points $[-\frac{3}{\sqrt{5}}, -\frac{1}{\sqrt{5}}, \frac{1}{\sqrt{5}}, \frac{3}{\sqrt{5}}]$ was carried out using a simulation using phase rotation of $\Delta = \frac{\pi}{4}$ and $\Delta = \frac{\pi}{3}$. In addition, a weight value was added to the codebook design with a value of w_1 = 0.6; w_2 = 0.3; and w_3 = 0.1 in the phase rotation of $\Delta = \frac{\pi}{4}$ and $\Delta = \frac{\pi}{3}$.

The simulation process for the SCMA system utilized four mapping matrix schemes. The first scheme employed a Latin-generating matrix with varying phases in rows or columns and a nonuniform weight value. The second scheme utilized a non-Latin generating matrix with consistent phase values in other rows or columns, also with a nonuniform weight value. The following are the utilized Latin matrices.

$$\boldsymbol{G}_{(4x6)}^{Lat} = \begin{bmatrix} \varphi_0 & \varphi_1 & \varphi_2 & 0 & 0 & 0 \\ \varphi_1 & 0 & 0 & \varphi_2 & \varphi_0 & 0 \\ 0 & \varphi_2 & 0 & \varphi_0 & 0 & \varphi_1 \\ 0 & 0 & \varphi_0 & 0 & \varphi_1 & \varphi_2 \end{bmatrix}.$$

The values of codebook design weighting on the Latin generator matrix with nonuniform codebook design weighting were w_1 = 0.6; w_2 = 0.3; and w_3 = 0.1.

$$\boldsymbol{G}_{(4x6)}^{PLat} = \begin{bmatrix} w_1.\varphi_0 & w_2.\varphi_1 & w_3.\varphi_2 & 0 & 0 & 0 \\ w_1.\varphi_1 & 0 & 0 & w_1.\varphi_2 & w_2.\varphi_0 & 0 \\ 0 & w_2.\varphi_2 & 0 & w_1.\varphi_0 & 0 & w_3.\varphi_1 \\ 0 & 0 & w_3.\varphi_0 & 0 & w_2.\varphi_1 & w_3.\varphi_2 \end{bmatrix}.$$

The third scheme, the non-Latin generation matrix, exhibits the inverse property of the Latin generation matrix. The following non-Latin matrices were used.

$$\boldsymbol{G}_{(4x6)}^{NLat} = \begin{bmatrix} \varphi_0 & \varphi_1 & \varphi_2 & 0 & 0 & 0 \\ \varphi_0 & 0 & 0 & \varphi_2 & \varphi_1 & 0 \\ 0 & \varphi_1 & 0 & \varphi_2 & 0 & \varphi_0 \\ 0 & 0 & \varphi_2 & 0 & \varphi_1 & \varphi_0 \end{bmatrix}.$$

The value of codebook design weighting on a non-Latin mapping matrix with nonuniform codebook design weighting was w_1 = 0.6; w_2 = 0.3; w_3 = 0.1.

$$\boldsymbol{G}_{(4x6)}^{PNLat} = \begin{bmatrix} w_1.\varphi_0 & w_2.\varphi_1 & w_3.\varphi_2 & 0 & 0 & 0 \\ w_1.\varphi_0 & 0 & 0 & w_1.\varphi_2 & w_2.\varphi_1 & 0 \\ 0 & w_2.\varphi_1 & 0 & w_1.\varphi_2 & 0 & w_3.\varphi_0 \\ 0 & 0 & w_3.\varphi_2 & 0 & w_2.\varphi_1 & w_3.\varphi_0 \end{bmatrix}$$

where φ_α is the phase rotation operating factor with a systematic form as in equation (9) [23].

$$\varphi_\alpha = e^{i.\alpha.\theta} \quad (9)$$

where α is an integer that meets $0 \leq \alpha \leq d_f - 1$. With a value of d_f = 3, there are α = 0, α = 1, and α = 2. The θ parameter is the interval of two adjacent constellation points. This study employed the $\Delta = \frac{\pi}{4}$ and $\Delta = \frac{\pi}{3}$ values.

III. RESULTS AND DISCUSSION

The results of the codebook design, obtained from the simulations, are presented in terms of BER values. This study simulated six users distributed across four resource elements. In conducting the simulation, each user generated six 4×4, codebook matrices, in which two resources were generated in each codebook matrix.

The graph in Figure 2 depicts the performance of BER using the basic line constellation on the AWGN channel. The results indicated that the optimal system performance was achieved with a $\frac{\pi}{3}$ phase rotation using a Latin generator, whereas a $\frac{\pi}{4}$ phase rotation employed a non-Latin generator. Specifically, the Latin generator with a $\frac{\pi}{3}$ phase rotation generates an SNR value of 6.96 dB, while the non-Latin generator with a $\frac{\pi}{4}$ phase rotation generates an SNR value of 10.38 dB at BER 10^{-3}.

The graph illustrates that Latin generators could enhance system performance on AWGN channels by eliminating errors present in SCMA codebooks. Consequently, this system could suppress overlap at the main constellation point in the most optimal $\frac{\pi}{3}$ phase. The non-Latin $\frac{\pi}{3}$ results indicated inferior system performance compared to others. This discrepancy arises because the probability value of the symbol detection error is greater, and the obtained minimum Euclidean value is smaller.

The graph depicted in Figure 3 illustrates the BER performance on the AWGN channel with the inclusion of weights. It demonstrates the optimal system performance in a $\frac{\pi}{3}$ phase rotation in both Latin and non-Latin. Specifically, at BER 10^{-1}, Latin generators exhibited an SNR value of 12.26 dB, while non-Latin generators exhibit an SNR of 12.28 dB.

The effect of adding weight to the AWGN channel altered the BER results from 10^{-3} to 10^{-1} and produced an intersystem curve image with negligible changes. It occurred because the resulting *dmin* value was smaller, leading to an increase in symbol detection error probabilities.

Figure 4 illustrates the performance of BER under Rayleigh fading. The results indicated that the system performance was

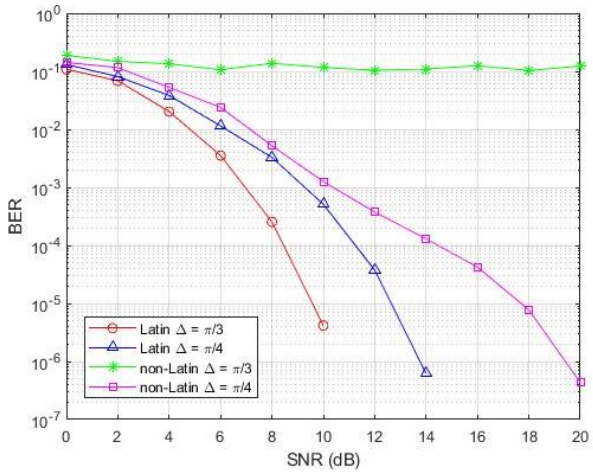

Figure 2. BER performance graph with basic line constellation on AWGN channel.

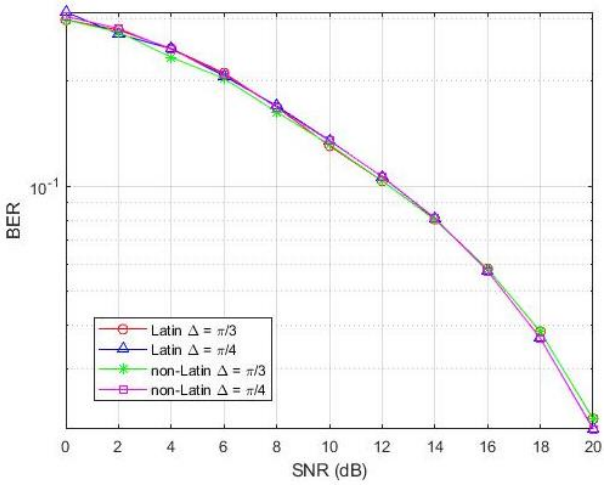

Figure 3. BER performance graph with the basic line constellation on the AWGN channel with the addition of weighting.

optimal with a $\frac{\pi}{4}$ phase rotation using Latin and non-Latin generators. Under a $\frac{\pi}{4}$ phase rotation, BER 10^{-3} resulted in an SNR value of 13.78 dB in Latin generators and an SNR of 13.73 dB in non-Latin generators.

The Latin generator did not function effectively in Rayleigh fading scenarios, and the most optimal system was inversely proportional to the AWGN channel. This phenomenon occurred due to the interference caused by Rayleigh fading on the transmitted signal conditions. Consequently, the results produced by the system did not demonstrate a significant difference between the tested systems.

Figure 5 illustrates the performance in Rayleigh fading with the incorporation of weights. The results demonstrated that the optimal system performance was achieved using a Latin generator with a $\frac{\pi}{3}$ phase rotation, while a non-Latin generator was optimal with a $\frac{\pi}{4}$ phase rotation. Specifically, at BER 10^{-1} SNR value of 13.8 dB was generated in the $\frac{\pi}{3}$ phase rotation of the Latin generator and SNR value of 14.3 dB in the $\frac{\pi}{4}$ phase rotation of the non-Latin generator. The introduction of weight to this Rayleigh fading altered the BER result from 10^{-3} to 10^{-1} and shifted the optimal data result in the Latin generator from $\frac{\pi}{4}$ to $\frac{\pi}{3}$.

Figure 6 illustrates the performance of BER using the basic line constellation on the Rician channel. Optimal system

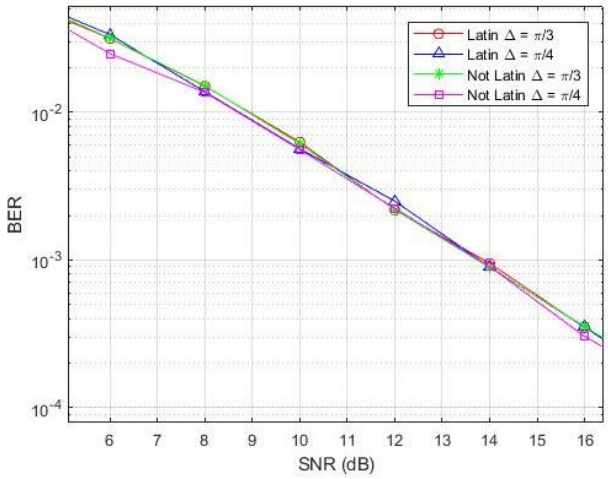

Figure 4. BER performance graph with baseband constellation in Rayleigh fading

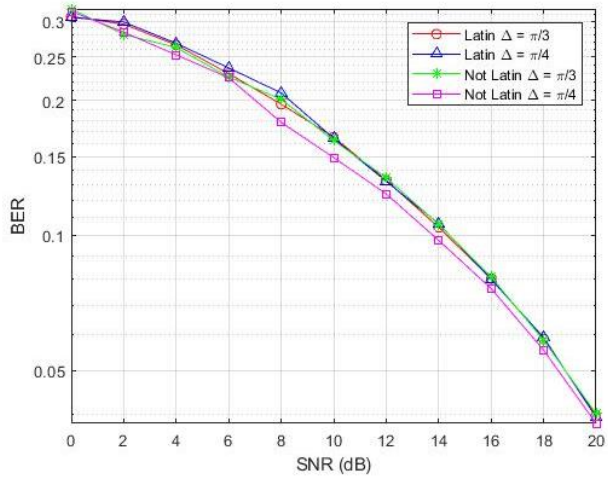

Figure 5. BER performance graph with basic line constellation in Rayleigh fading with added weighting

performance is indicated by a $\frac{\pi}{4}$ phase rotation in both Latin and non-Latin generators. A BER 10^{-6} in a $\frac{\pi}{4}$ phase rotation resulted in an SNR value of 8.91 dB in the Latin generator and an SNR value of 8.88 dB in the non-Latin generator. In the Rician channel, the non-Latin $\frac{\pi}{4}$ configuration did not yield a BER value. The results in this Rician channel showed no significant differences between systems because the transmitted signals were disrupted.

Figure 7 illustrates the BER performance utilizing the basic line constellation in the Rician channel with the addition of weight. Optimal system performance is indicated by a $\frac{\pi}{4}$ phase rotation using Latin and non-Latin generators. A BER 10^{-3} in a $\frac{\pi}{4}$ phase rotation resulted in an SNR value of 15.15 dB in the Latin generator and an SNR value of 15.2 dB in the non-Latin generator. The introduction of weight to the Rician channel altered the BER outcome from 10^{-6} to 10^{-3} and converted the optimal generator from non-Latin $\frac{\pi}{4}$ to Latin $\frac{\pi}{4}$.

Figure 8 illustrates a comparison of phase and weighting in the AWGN channel, Rayleigh fading, and Rician channel. The optimal results were observed in the AWGN channel with A value of 10^{-3} at SNR 9.42 dB. In contrast, there was no significant difference between the Rician channel and Rayleigh fading, both achieving optimal performance with a value of 10^{-3} at SNR 12.81 dB and 14.47 dB, respectively.

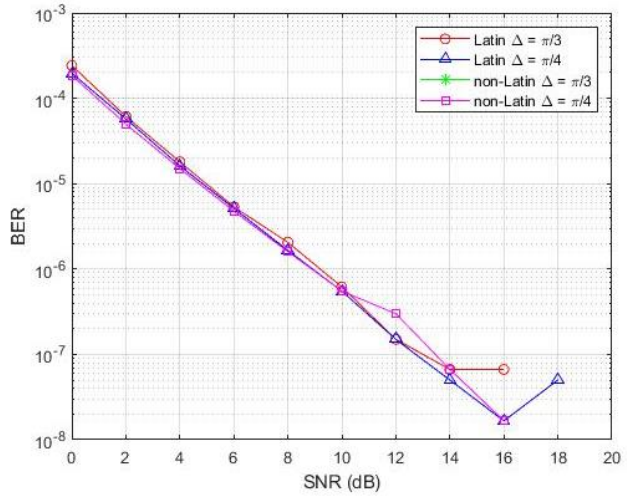

Figure 6. BER performance chart with the basic line constellation on the Rician channel.

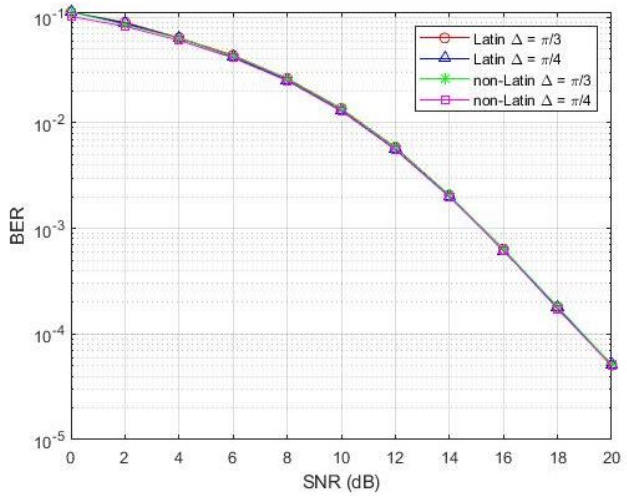

Figure 7. BER performance graph with the basic line constellation on the Rician channel with the addition of weights.

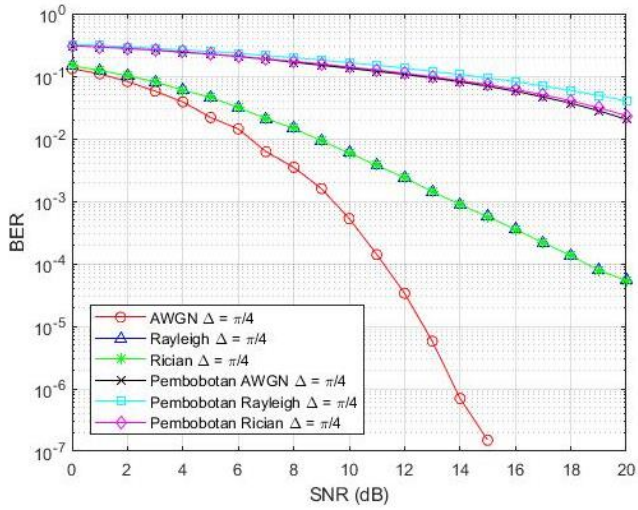

Figure 8. BER performance graph with phase comparison on the three channels.

Based on the obtained data, this weighting had the most significant impact on the system in the AWGN channel, resulting in a BER value of 10^{-1} at SNR 12.48 dB. The second most affected channel was the Rician channel, exhibiting a BER value of 10^{-1} at SNR 12.81 dB. The third significant result occurred in Rayleigh fading, with a BER value of 10^{-1} at SNR 14.47 dB.

IV. CONCLUSION

The design of the appropriate codebook design is the primary factor determining the performance of the SCMA system. SCMA systems require basic constellation, phase rotation variation, and generator matrix variation. Optimal Euclidean minimum distances in the constellation may improve BER performance, while phase rotation may affect power variation by maintaining Euclidean minimum distances.

The results of the optimal codebook design were obtained in the non-Latin Rician $\frac{\pi}{4}$ channel with BER 10^{-6} and SNR 8.88 dB, achieving a minimum Euclidean distance of 0.3423. Conversely, the codebook design of weighting took place in the Rician channel with A value of 10^{-3} and SNR 15.15 dB in Latin $\frac{\pi}{4}$ with a minimum Euclidean distance of 0.0894. Among the two generators, the Latin generator was found to enhance system performance.

From the phase comparison across the three channels, optimal results were obtained in the AWGN channel with a BER value of 10^{-3} at SNR 9.42 dB. However, no significant difference was observed in the Rician channel and Rayleigh fading scenarios.

The effect of weighting on the line modulation constellation resulted in a decrease in both the minimum Euclidean and the average energy at the lower point. Additionally, the effect on the minimum Euclidean distance and the average energy of the point brought these distances closer together, resulting in similar values for both phases. This weighting demonstrates its most significant influence in the AWGN channel, yielding a BER value of 10^{-1} and an SNR of 12.48 dB.

In this study, no significant changes were observed between systems, particularly in the design of codebooks with additional weight. Therefore, future research should encompass a wider range of weighting values, modulation types, phase rotation values, and modulation constellations.

CONFLICTS OF INTEREST

This paper is free from any conflicts of interest.

AUTHORS' CONTRIBUTIONS

Conceptualization, Linda Meylani; methodology, Linda Meylani; software, Shilvy Fatma; validation, Vincent Sigit; formal analysis, Shilvy Fatma, Linda Meylani; resources, Linda Meylani; original drafting, Shilvy Fatma; reviewing, Vincent Sigit.

REFERENCES

[1] S. Khan *et al.*, "Highly accurate and reliable wireless network slicing in 5th generation networks: A hybrid deep learning approach," *J. Netw. Syst. Manag.*, vol. 30, no. 2, pp. 1–22, Jan. 2022, doi: 10.1007/s10922-021-09636-2.

[2] A.E. Grant and J. Meadows, Eds, *Communication Technology Update and Fundamentals*, 17th ed. New York, NY, USA: Routledge, 2020.

[3] B. Clerckx *et al.*, "A primer on rate-splitting multiple access: Tutorial, myths, and frequently asked questions," *IEEE J. Sel. Areas Commun.*, vol. 41, no. 5, pp. 1265–1308, May 2023, doi: 10.1109/JSAC.2023.3242718.

[4] L. Zhu, Z. Xiao, X.-G. Xia, and D.O Wu, "Millimeter-wave communications with non-orthogonal multiple access for B5G/6G," *IEEE Access*, vol. 7, pp. 116123–116132, Aug. 2019, doi: 10.1109/ACCESS.2019.2935169.

[5] C.B. Mwakwata *et al.*, "Cooperative scheduler to enhance massive connectivity in 5G and beyond by minimizing interference in OMA and NOMA," *IEEE Syst. J.*, vol. 16, no. 3, pp. 5044–5055, Sep. 2022, doi: 10.1109/JSYST.2021.3114338.

[6] M. Ligwa and V. Balyan, "A comprehensive survey of NOMA-based cooperative communication studies for 5G implementation," in *Expert Clouds and Applications*, I.J. Jacob, F.M. Gonzalez-Longatt, S.K.

Shanmugam, I. Izonin, Eds., Singapore, Singapore: Springer, 2021, pp. 619–629, doi: 10.1007/978-981-16-2126-0_49.

[7] M. Hassan, M. Singh, and K. Hamid, "BER performance of NOMA downlink for AWGN and Rayleigh fading channels in (SIC)," *EAI Endorsed Trans. Mobile Commun. Appl.*, vol. 7, no. 21, pp. 1–7, Jun. 2022, doi: 10.4108/eai.20-6-2022.174227.

[8] H. Nikopour and H. Baligh, "Sparse code multiple access," *2013 IEEE 24th Annu. Int. Symp. Pers. Indoor Mobile Radio Commun. (PIMRC)*, 2013, pp. 332–336, doi: 10.1109/PIMRC.2013.6666156.

[9] A. Sultana *et al.*, "Efficient resource allocation in SCMA-enabled device-to-device communication for 5G networks," *IEEE Trans. Veh. Technol.*, vol. 69, no. 5, pp. 5343–5354, May 2020, doi: 10.1109/TVT.2020.2983569.

[10] W.B. Ameur *et al.*, "Performance study of MPA, Log-MPA and MAX-Log-MPA for an uplink SCMA scenario," *2019 26th Int. Conf. Telecommun. (ICT)*, 2019, pp. 411–416, doi: 10.1109/ICT.2019.8798841.

[11] X. Zhang *et al.*, "An efficient SCMA codebook design based on lattice theory for information-centric IoT," *IEEE Access*, vol. 7, pp. 133865–133875, Aug. 2019, doi: 10.1109/ACCESS.2019.2938637.

[12] K. Hassan, K. Raoof, and P. Chargé, "Multi-dimensional codebooks for multiple access schemes," in *Coding Theory Essent*, D. Harkut, K.N Kasat, Eds., London, United Kingdom: IntechOpen, 2023, doi: 10.5772/intechopen.110032.

[13] Y. Zhou, Q. Yu, W. Meng, and C. Li, "SCMA codebook design based on constellation rotation," *2017 IEEE Int. Conf. Commun. (ICC)*, 2017, pp. 1–6, doi: 10.1109/ICC.2017.7996395.

[14] R. Hoshyar, F.P. Wathan, and R. Tafazolli, "Novel low-density signature for synchronous CDMA systems over AWGN channel," *IEEE Trans. Signal Process.*, vol. 56, no. 4, pp. 1616–1626, Apr. 2008, doi: 10.1109/TSP.2007.909320.

[15] M. Kulhandjian, H. Kulhandjian, C. D'amours, and L. Hanzo, "Low-density spreading codes for NOMA systems and a Gaussian separability-based design," *IEEE Access*, vol. 9, pp. 33963–33993, Feb. 2021, doi: 10.1109/ACCESS.2021.3060879.

[16] M. Jia, S. Meng, Q. Guo, and X Gu, "Design of codebook for high overload SCMA," in *Communications, Signal Processing, and Systems – CSPS 2019*, Q. Liang, W. Wang, X Liu, Z. Na, M. Jia, B. Zhang, Eds., Singapore, Singapore: Springer, 2020, pp. 2654–2662, doi:10.1007/978-981-13-9409-6_324.

[17] R. Thirunavukkarasu, R. Balasubramanian, and V. Bhaskar, "An optimum probabilistic shaping based uplink SCMA codebook design using hybrid firefly-bat algorithm," *Wireless Pers. Commun.*, vol. 130, no. 1, pp. 527–549, May 2023, doi: 10.1007/s11277-023-10297-4.

[18] Y.M. Tabra and B.M. Sabbar, "New computer generated-SCMA codebook with maximized Euclidian distance for 5G," *Iraqi J. Inf. Commun. Technol. (IJICT)*, vol. 2, no. 2, pp. 9–24, Jun. 2019, doi: 10.31987/ijict.2.2.64.

[19] D.A. Pokamestov, Y.V. Kryukov, E.V. Rogozhnikov, and I. Kanatbekuli, "Adapting SCMA codebooks to channel state," *2021 3rd Int. Youth Conf. Radio Electron. Electr. Power Eng. (REEPE)*, 2021, pp. 1–4, doi: 10.1109/REEPE51337.2021.9388063.

[20] Q. Luo *et al.*, "A design of low-projection SCMA codebooks for ultra-low decoding complexity in downlink IoT networks," *IEEE Trans. Wireless Commun.*, vol. 22, no. 10, pp. 6608–6623, Oct. 2023, doi: 10.1109/TWC.2023.3244868.

[21] M. Rebhi, K. Hassan, K. Raoof, and P. Chargé, "Sparse code multiple access: Potentials and challenges," *IEEE Open J. Commun. Soc.*, vol. 2, pp. 1205–1238, May 2021, doi: 10.1109/OJCOMS.2021.3081166.

[22] Z. Qin, Y. Su, R. Liu, and C. Liu, "Codebook optimization design of serial encoding SCMA system," *2022 Int. Symp. Netw. Comput. Commun. (ISNCC)*, 2022, pp. 1–4, doi: 10.1109/ISNCC55209.2022.9851751.

[23] Z. Hou, Z. Xiang, P. Ren, and B. Cao, "SCMA codebook design based on decomposition of the superposed constellation for AWGN channel," *Electron.*, vol. 10, no. 17, pp. 1–10, Aug. 2021, doi: 10.3390/electronics10172112.